Oil Production Optimization of Black-Oil Models by Integration of Matlab and Eclipse E300

Hørsholt, Steen; Nick, Walker,; Jørgensen, John Bagterp

Published in:
IFAC-PapersOnLine

Link to article, DOI:
10.1016/j.ifacol.2018.06.360

Publication date:
2018

Document Version
Publisher's PDF, also known as Version of record

Available online at www.sciencedirect.com

ScienceDirect

IFAC Papers Online CONFERENCE PAPER ARCHIVE

IFAC PapersOnLine 51-8 (2018) 88–93

Oil Production Optimization of Black-Oil Models by Integration of Matlab and Eclipse E300 ⋆

S. Hørsholt *, **H.M. Nick** **, **J.B. Jørgensen** *

* *Department of Applied Mathematics and Computer Science & Center for Energy Resources Engineering (CERE), Technical University of Denmark, DK-2800 Kgs. Lyngby, Denmark.*
** *Danish Hydrocarbon Research and Technology Centre, Technical University of Denmark, DK-2800 Kgs. Lyngby, Denmark*

Abstract: In this paper, we present a software tool for oil production optimization. The software combines the simulation power of a commercial black-oil reservoir simulator with adjoint-gradient capability (Eclipse E300) and state-of-the-art software for constrained optimization (Matlab). The software enables deterministic and ensemble-based optimization strategies for black-oil reservoir flow models and compositional reservoir flow models. The software implements a number of ensemble-based optimization strategies such as the robust optimization, the mean-variance optimization, and the conditional value at risk optimization. Consequently, the software constitutes a powerful tool to assist and guide decision making in the real-life reservoir management process. In this paper, we present the workflow and numerical results for mean-variance optimization of a synthetic 2-dimensional black-oil reservoir using water flooding.

Keywords: Black-oil model, Production optimization, Reservoir management, Workflow

1. INTRODUCTION

In an unstable low price market with strict environmental regulations, implementation of life-cycle production optimization methods for reservoir management receives growing interest from the industry (Hanea et al., 2016; Leeuwenburgh et al., 2016; Jansen et al., 2009; Hou et al., 2015; Oliveira and Reynolds, 2015). To increase profits and mitigate risk in production of maturing fields, the industry calls for recovery methods that increases production with low risk and little environmental impact. Oil production optimization of water flooded oil fields can prove to be such a method (Brouwer et al., 2004; van Essen et al., 2009; Foss, 2012; Rahmawati et al., 2012; Sarma et al., 2008; Wang et al., 2009; Völcker et al., 2011; Capolei et al., 2013). Many existing fields are in the second or third stage of recovery, where the infrastructure for water flooding is already in-place. Thus, the cost of incorporating production optimization in the operating strategy decisions is relatively low. Ensemble-based methods have been a focal point in the literature to account for the inherent geological uncertainty of the subsurface (van Essen et al., 2009; Peters et al., 2010). Black-oil models are widely used throughout the industry for simulation and prediction. These simulations and predictions serve as a decision support tool for the management. To further assist the management in making *optimal* decisions requires that the simulation and predictions are combined with optimization methods. Consequently, routinely appilcation of oil production optimization methods in the industry requires that research efforts are extended from simple small-scale two-phase reservoir flow models to real size reservoir geometry as well as black-oil flow models. The complexity and size of typical industry reservoir models necessitate user-friendly, fast, reliable and robust reservoir simulators. In this paper, we combine ensemble-based optimization methods, a black-oil reservoir flow model, and a commercial reservoir simulation tool to enable realistic industrial scale production optimization.

Oil production optimization research as described in the literature is for a large part limited to two-phase immiscible flow in synthetic reservoir models, simulated in various open source, research purpose or in-house reservoir simulators (Hou et al., 2015). Through years of development and use, commercial simulators have obtained flexibility, computational speed, and robustness. For this reason, most oil companies creates simulations models of their reservoirs in an industry standard commercial simulator. Chen et al. (2010) and Asadollahi and Naevdal (2009) both applied gradient-based optimization on the synthetic two-phase Brugge field (Peters et al., 2010) using a commercial reservoir simulator (E300). Demonstration of ensemble-based optimization methods on realistic reservoirs simulated with black-oil flow models will help to bring the research closer to a point where the industry is willing to implement such methods into the reservoir management workflow. The large number of simulations required in ensemble-based optimization methods necessitates the use of gradient-based optimization for the methods to be computationally feasible. This implies that ensemble-based production optimization for an industry scale reservoir is

⋆ This research is funded by the Danish Hydrocarbon Research and Technology Centre under the Advanced Water Flooding programme.

10.1016/j.ifacol.2018.06.360

only practically feasible, if the reservoir simulator is able to compute the gradient, e.g. by the adjoint method.

In this paper, we present a workflow that combines the robustness, simulation power and adjoint capability of a well-established commercial reservoir simulator (Schlumberger E300) and state-of-the-art optimization algorithms (Matlab) to provide a robust gradient-based optimization tool (RESOPT). The optimization strategies implemented in the software tool are the ensemble-based methods: robust optimization, mean-variance optimization, and conditional value at risk optimization. In this paper, we only consider the mean-variance optimization method. This software integration enables reservoir engineers to routinely use existing realistic black-oil reservoir flow models implemented in Eclipse for ensemble-based production optimization.

The structure of the paper is as follows. Section 2 describes the black-oil flow-model, the net present value objective, and the optimal control problem to be solved. Section 3 describes the ensemble-based mean-variance optimization problem. The workflow in the production optimization software tool is described in Section 4. Section 5 presents a case study of a mean-variance optimization of a synthetic 2-dimensional black-oil reservoir. Conclusions are provided in section 6.

2. RESERVOIR SIMULATOR

In this section, we state the black-oil model equations for flow in porous media and the net present value objective function. The aim is not to give a detailed description of any specific numerical implementation of the black-oil model, but to give an outline of the mathematical features a reservoir simulator should implement to be suited for computationally efficient production optimization. Aziz and Durlofsky (2005) and Chen et al. (2006) provide a thorough description of the black-oil model.

2.1 Black-oil model for flow in porous media

The basic black-oil model for live oil and dry gas can be derived from the general multiphase flow model using the following assumptions about the fluid mixture. 1) The mixture consists of water (W), oil (O), and gas (G). 2) The mixture has a water phase (w), an oil phase (o), and a gas phase (g). 3) The water and oil components exists only in their corresponding phases. The gas component exists both in the gas phase and in the oil phase.

The black-oil mass-balance differential equations are

$$\frac{\partial}{\partial t}C_\beta = -\nabla \cdot N_\beta + Q_\beta, \quad \beta \in \{W, O, G\}. \tag{1}$$

For each phase, the concentrations, fluxes, and source/sink terms are given by: $C_W = \phi\rho_w S_w$, $N_W = \rho_w \mathbf{u}_w$, $Q_W = \rho_w q_{Ws}$, $C_O = \phi\rho_{Oo} S_o$, $N_O = \rho_{Oo}\mathbf{u}_o$, $Q_O = \rho_o q_{Os}$, $C_G = \phi(\rho_{Go} S_o + \rho_g S_g)$, $N_G = \rho_{Go}\mathbf{u}_o + \rho_g \mathbf{u}_g$, $Q_G = \rho_g q_{Gs}$. ϕ denotes the porosity of the porous media. The saturation, density and Darcy velocity of a phase, $\alpha \in \{w, o, g\}$, are denoted by S_α, ρ_α, and $\mathbf{u}_\alpha$, respectively. $q_{\beta s}$ denotes the component surface flow rates. In addition, phase equilibrium conditions determines the distribution of the gas component (G) between the gas phase (g) and the oil phase (o). Furthermore, the saturations of the phases (S_w, S_o, S_g) are related by the volume constraint $S_w + S_o + S_g = 1$. The pressures of the different phases (P_w, P_o, P_g) are related by the capilary pressures, $P_{cow} = P_o - P_w$ and $P_{cgo} = P_g - P_o$.

2.2 Discretization

Most reservoir simulators discretize the flow equations in space by a finite-volume method and in time by the implicit Euler method. We denote the state vector as $x(t) \in \mathbb{R}^{n_x}$, the vector of manipulated variables as $u(t) \in \mathbb{R}^{n_u}$, and the vector of geological parameters as θ. $u(t)$ is discretized by a zero-order-hold defined by $u(t) = u_k, t_k \leq t \leq t_{k+1}, k = 0, \ldots, N-1$, where $t_N = t_f$ is the final time.

After spatial and temporal discretization, we write the black-oil model as the system of nonlinear equations

$$R_k = R(x_{k+1}, x_k, u_k; \theta) = 0, \ k = 0, 1, \ldots, N-1. \tag{2}$$

Using a Matlab-like notation we introduce the vectors $\bar{x} = (x_1; x_2; \ldots; x_N)$, $\bar{R} = (R_0; R_1; \ldots; R_{N-1})$, and $\bar{u} = (u_0; u_1; \ldots; u_{N-1})$. This allows us to express the residual equations (2) compactly as

$$\bar{R}(\bar{x}, \bar{u}, x_0; \theta) = 0. \tag{3}$$

2.3 Net present value

The net present value over the life time of an oil reservoir can be defined as a function, Φ, of the states, $\bar{x}$, the operating trajectory, $\bar{u}$, the initial state, x_0, and the the geological parameters, θ. The net present value is in discrete time written as

$$\Phi(\bar{x}, \bar{u}, x_0; \theta) = \sum_{k=0}^{N-1} J_k(x_{k+1}, u_k; \theta), \tag{4}$$

where the discounted net present value, J_k, for the k'th time interval is given by

$$J_k = \frac{\Delta t_k}{(1+d)^{t_{k+1}/t_\tau}} \Big[r_o q_{Os,k+1} + r_g q_{Gs,k+1} - (r_w q_{Ws,k+1} + r_{w,\text{inj}} q_{w,\text{inj},k+1}) \Big]. \tag{5}$$

Δt_k, is the length of the k'th time interval, d is the annual discount factor, t_τ is the discount time interval. r_o and r_g are the sale prices for oil and gas. r_w is the water production cost and $r_{w,\text{inj}}$ is the water injection cost. The corresponding flow rates for oil, gas, water, and water injection are denoted as, $q_{Os}, q_{Gs}, q_{Ws}, q_{w,\text{inj}}$.

2.4 Optimal control problem

The discrete-time constrained optimal control problem for production optimization is given by (Capolei et al., 2012)

$$\max_{\bar{u} \in \mathcal{U}} \quad \psi = \psi(\bar{u}; x_0, \theta), \tag{6}$$

where the objective function is

$$\psi(\bar{u}; x_0, \theta) = \Big\{ \Phi(\bar{x}, \bar{u}, x_0; \theta) : \bar{R}(\bar{x}, \bar{u}, x_0; \theta) = 0 \Big\}. \tag{7}$$

In this paper, only linear constraints on the input are considered. The constraints are lower/upper bounds on controls, rate of movement constraints on controls to prevent 'large' changes in rates/bhp's, and upper/lower

bounds on total injection rates in each time step. The constraints are written as $\mathcal{U} = \{\bar{u} : \bar{u}_{\min} \leq \bar{u} \leq \bar{u}_{\max}, \Delta\bar{u}_{\min} \leq \Delta\bar{u} \leq \Delta\bar{u}_{\max}, b_l \leq \bar{A}\bar{u} \leq b_u\}$.

2.5 Black-box reservoir simulator

In this paper, we introduce an optimization workflow that is not reliant on any specific formulation nor solution method of the black-oil flow equations (1). Accordingly, we treat the reservoir simulator as a black-box function. To be suited for production optimization, a reservoir simulator must satisfy the following requirements. Given the initial state, x_0, an operating profile, $\bar{u}$, and a geological realization vector, θ, it must at all subsequent time-steps return the states, $\bar{x}$, the net present value, ψ, and the gradient of the net present value with respect to the controls, $\nabla_{\bar{u}}\psi$. We denote this black-box simulation function, $\mathcal{S}$, as

$$[\bar{x}, \psi, \nabla_{\bar{u}}\psi] = \mathcal{S}(\bar{u}; x_0, \theta). \tag{8}$$

3. ENSEMBLE-BASED OPTIMIZATION

In this section, we describe the ensemble-based mean-variance optimization strategy for the net present value of a reservoir under geological uncertainty. The ensemble-based mean-variance optimization strategy optimizes a bi-criterion objective function consisting of a convex combination of the mean and the variance of the net present value.

3.1 Mean-variance optimization

In ensemble-based methods, the idea is to represent the uncertainty associated with the geological parameters in an ensemble of equally probable realizations, $\theta^{n_\theta} = \{\theta_i\}_{i=1}^{n_\theta}$. The corresponding ensemble of net present values for a given initial condition, x_0, and operating profile, $\bar{u}$, is $\{\psi^i\}_{i=1}^{n_\theta}$, where $\psi^i = \psi(\bar{u}; x_0, \theta_i)$.

The mean-variance optimization strategy aims to combine the conflicting objectives of increasing the mean net present value while lowering the associated risk measured as the variance of the net present value. The mean-variance optimization problem is

$$\max_{\bar{u}\in\mathcal{U}} \quad \psi_{MVO}(\bar{u}; x_0, \theta^{n_\theta}), \tag{9}$$

where the objective function,

$$\psi_{MVO} = \lambda\psi_{RO} - (1-\lambda)\psi_{\sigma^2}, \tag{10}$$

is a convex combination of the mean, ψ_{RO}, and the variance, ψ_{σ^2}, for the trade-off parameter, $\lambda \in [0, 1]$. The mean, ψ_{RO}, and the variance, ψ_{σ^2}, are computed as their ensemble sample estimates:

$$\psi_{RO} = \frac{1}{n_\theta}\sum_{i=1}^{n_\theta}\psi^i, \tag{11a}$$

$$\psi_{\sigma^2} = \frac{1}{n_\theta - 1}\sum_{i=1}^{n_\theta}\left(\psi^i - \psi_{RO}\right)^2. \tag{11b}$$

The gradient of the mean-variance objective (10) is given as a combination of the gradients of the individual net present value ensemble members, $\nabla_{\bar{u}}\psi^i$:

$$\nabla_{u_k}\psi_{MVO} = \lambda\nabla_{u_k}\psi_{RO} - (1-\lambda)\nabla_{u_k}\psi_{\sigma^2}, \tag{12a}$$

$$\nabla_{u_k}\psi_{RO} = \frac{1}{n_\theta}\sum_{i=1}^{n_\theta}\nabla_{u_k}\psi^i, \tag{12b}$$

$$\nabla_{u_k}\psi_{\sigma^2} = \frac{2}{n_\theta - 1}\sum_{i=1}^{n_\theta}(\psi^i - \psi_{RO})\nabla_{u_k}\psi^i. \tag{12c}$$

This implies that the objective, ψ_{MVO}, and the gradient, $\nabla_{\bar{u}}\psi_{MVO}$, may be computed by computing the objective, ψ^i, and the gradient, $\nabla_{\bar{u}}\psi^i$, for each ensemble member, i.e. $\{\psi^i, \nabla_{\bar{u}}\psi^i\}_{i=1}^{n_\theta}$. These computations are conducted in parallel by the reservoir simulator, i.e. $[\bar{x}^i, \psi^i, \nabla_{\bar{u}}\psi^i] = \mathcal{S}(\bar{u}; x_0, \theta^i)$ for $i = 1, 2, \ldots, n_\theta$.

4. WORKFLOW

In this section, we outline the workflow for RESOPT. RESOPT is a workflow management tool for production optimization that integrates Eclipse (E300) and Matlab. The Eclipse file-format is the base of the software integration. Matlab manages the data processing and communication between the optimizer and the external simulator. The optimizer is `fmincon` from Matlab's optimization toolbox. Eclipse E300 is used as the reservoir simulator because it is well-established and can compute the gradients using the adjoint method.

4.1 Overview of workflow

Fig. 1 illustrates the workflow in the RESOPT software. The parameters defining the optimization problem are supplied by the user in the script `defineOptModel` that follows a specific template. The production optimization computations are started from the driver script `optimizeModel`. This script calls `defineOptModel` to collect the user-defined parameters and passes them to the optimizer, `fmincon`. The optimizer calls the function `runOptimizationStrategy` that manages the communication with the external simulator through the function `runModel`. `runOptimizationStrategy` calls the simulator with a given production strategy, $\bar{u}$, and a given realization of the parameters, θ_i, for all realizations in the ensemble, $i = 1, 2, \ldots, n_\theta$. The reservoir simulator computes and return the states, $\bar{x}$, the net present value, ψ^i, and the gradients, $\nabla_{\bar{u}}\psi^i$. For a cluster of computers, these calls to the simulator may be conducted in parallel. We note that for ensemble-based strategies on industry-scaled reservoirs, access to a high-performance computing cluster is essential for the optimization to be computationally tractable. Given $\{\psi^i, \nabla_{\bar{u}}\psi^i\}_{i=1}^{n_\theta}$, `runOptimizationStrategy` computes the objective value and the gradients of the chosen strategy, e.g. ψ_{MVO} and $\nabla_{\bar{u}}\psi_{MVO}$, and returns these values to the optimizer, `fmincon`. Based on the returned information, the optimizer checks for convergence. If $\bar{u}$ is not optimal, the optimizer computes a new iterate, $\bar{u}$. The procedure is repeated until the optimizer has converged to a set of optimal controls, $\bar{u}$.

After convergence, the software saves all iteration data in a folder, together with the optimal simulation results for each member of the ensemble. To enable the reservoir engineer to monitor the optimization process, a dashboard displays relevant optimization and production data from

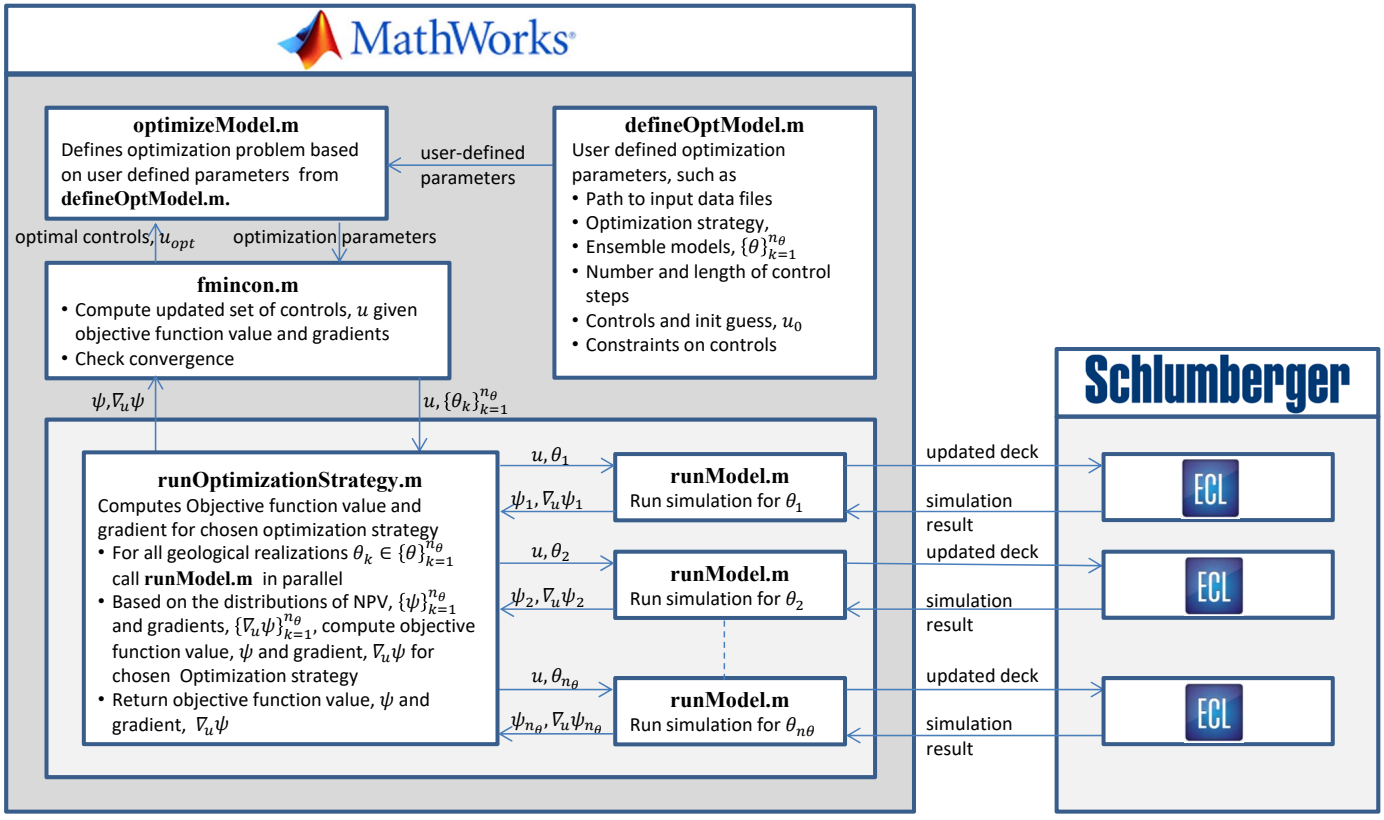

Fig. 1. Flowchart showing the workflow in the RESOPT optimization software.

the simulation. The controls, $\bar{u}$, and the gradients of the objective, $\nabla_{\bar{u}}\psi$, are divided between injectors and producers. At each optimization iteration, the objective function value, ψ, is appended in the dashboard. Also the controls, the gradients, and the net present value are updated along with selected production data. The selected data can be any type of time dependent results based on output from the simulation.

4.2 User-defined optimization parameters

The parameters stated in `defineOptModel` are divided into two main types, namely model parameters (see Table 2) and optimization parameters (see Table 3). The optimization parameters control the optimizer, e.g. the choice of optimization algorithm, the convergence tolerances, the maximum number of iterations, etc. The model parameters define the optimization problem, e.g. the number and the length of control time-steps, the choice of controlled parameters, the starting guess for the controls, the constraints on controls, the choice of optimization strategy, the size of the ensemble, the fluid prices, the discount factor, the scaling, etc.

5. CASE STUDY

In this section, we present a case study that demonstrates the use of the RESOPT optimization tool. The case study is a mean-variance optimization of a water flooded synthetic 2-dimensional black-oil reservoir model. An ensemble of 30 realizations represents the geological uncertainty associated with the permeability field.

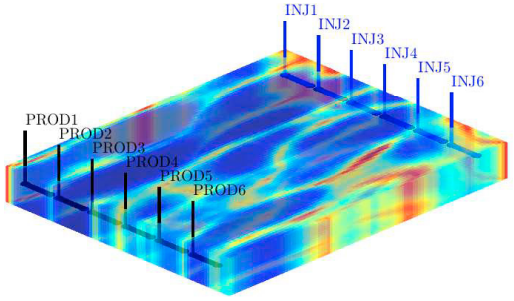

Fig. 2. Well locations and permeability field of the first realization in the synthetic two-dimensional black-oil case study.

5.1 2-Dimensional synthetic reservoir model

To test the optimization tool, we have created a two-dimensional synthetic reservoir model with a highly channeled isotropic permeability field. Fig. 2 shows the synthetic reservoir with the first realization of the permeability field and the well locations. The synthetic reservoir model has the physical dimensions $(800 \times 1000 \times 10)$ m and is discretized into an equidistant $(80, 100, 1)$ Cartesian grid. The ensemble permeability fields scales to a range of 0-1200 mD. The reservoir has 12 horizontal wells, consisting of 6 water injectors and 6 producers. The injectors are located in-line from south to north close to the eastern boundary of the reservoir. The producers are located opposite along the western boundary. The reservoir fluid is of a black-oil type. Table 1 shows the reservoir data. The reservoir has an initial water saturation of 0.2 and an oil saturation of 0.8.

Table 1. Reservoir data.

Description	symbol	value	metric
physical dim	(x, y, y)	$(800, 1000, 10)$	[m]
grid-cell dim	$(\Delta x, \Delta y, \Delta z)$	$(10, 10, 10)$	[m]
porosity, uniform	ϕ	0.2	-
water compressibility	c_w	1.45e-5	[bar^{-1}]
rock compressibility	c_r	4.35E-10	[bar^{-1}]
capillary pressure	P_c	0	[bar]
pore volume	V_{pore}	1.6e6	[m^3]
oil in place	V_{oip}	1.28e6	[m^3]
permeability range	(k_x, k_y)	$[0, 1200]$	[mD]
bubble-point pressure	P_b	153.67	[bar]
datum press	P_r	130.00	[bar]
datum depth	d_r	1500.00	[m]
oil water contact	OWC	2000.00	[m]
gas-oil contact	GOC	1000.00	[m]
initial water saturation	S_{wi}	0.2	-

Table 2. Model parameters.

Description	symbol	value	metric
strategy	MVO	-	-
number of realizations	n_θ	30	-
trade-off parameter	λ	$0, \ldots, 1.0$	-
simulation time	t_f	3600	[day]
number of control steps	N	120	-
length of control steps	Δt	30	[day]
number of controlled wells	n_w	6	-
number of controls	n_u	720	-
initial controls	u_{init}	62.5	[m^3/day]
lower bound on controls	$u_{\min}$	0.01	[m^3/day]
upper bound on controls	$u_{\max}$	250.0	[m^3/day]
rom constraint	b_l, b_i	30	[m^3/day]
total bounds on injectors	b_u	750	[m^3/day]
discount factor	d	0.08	-
fluid prices: oil	r_o	283.04	[US\$/m^3]
gas	r_g	0.0036	[US\$/m^3]
water	r_w	62.90	[US\$/m^3]
water injection	$r_{w,inj}$	12.58	[US\$/m^3]

5.2 Numerical results for mean-variance optimization

We have performed a number of mean-variance optimizations of the 2-dimensional reservoir for the trade-off parameter, $\lambda = 0.0, 0.1, \ldots, 1.0$, in-order to compute the Pareto frontier (Capolei et al., 2015). The reservoir is simulated for $t_f = 3600$ days with $N = 120$ control time-steps of equal length, $\Delta t = 30$ days. The optimizer manipulates the water injection rates to obtain the maximum mean-variance net present value. It uses 62.5 m^3/day as a starting iterate for the water injection. The individual injection rates are bounded in the interval [0.1, 250] m^3/day and have a rate of movement constraint of ± 30m^3 between control steps (per 30 days). The total injection rate of all water injectors combined is restricted to a maximum of 750 m^3/day. The bottom-hole pressure is kept constant at 125 bar in all producer wells throughout the simulation. The discount rate, d, is set to 8% annually. Optimization is performed using the interior-point algorithm in `fmincon`. Table 2 shows the model parameters and Table 3 shows the optimization parameters used in the optimization.

Fig. 3 shows the dashboard after convergence for the trade-off parameter $\lambda = 0.3$. The dashboard shows the operating profile (controls), the gradient of the objective w.r.t. the controls, the objective value, and the mean net present value together with the lowest and highest outcome. The figure shows how the cash flow shifts towards the early reservoir life. The net present value reaches 95 percent of the optimal value after only 1350 days of production. The optimizer converges after 91 iterations and 117 function evaluations.

Table 3. Optimization parameters.

Description	symbol	value	metric
algorithm	interior point	-	-
max iterations	maxit	100	-
max function evaluations	maxit	1000	-
tolerance on optimimality	tol_{opt}	10^{-6}	-
tolerance on step size	$\text{tol}_{\Delta u}$	10^{-6}	[m^3/day]

For any choice of the trade-off parameter, λ, the optimization result is a Pareto-optimal solution. We note that for $\lambda = 0$ and $\lambda = 1$ this corresponds to a variance optimization and a robust optimization, respectively. Fig. 4 shows the computed efficient frontier. The figure shows that the front is close to being monotonously increasing. This implies that increasing return comes with increasing risk.

6. CONCLUSION

We have developed software, RESOPT, for production optimization that manages the workflow between reservoir simulation and numerical optimization. In this paper, we applied RESOPT to production optimization of a reservoir described by a black-oil model using an ensemble-based mean-variance optimization criterion. RESOPT uses Eclipse (E300) for reservoir simulation, computation of the net present value, and computation of the gradient of the net present value. By using an industry standard simulator such as Eclipse, model based production optimization is brought a step closer to routinely implementation in closed-loop oil reservoir management.

REFERENCES

Asadollahi, M. and Naevdal, G. (2009). Waterflooding optimization using gradient based methods. *SPE/EAGE Reservoir Characterization & Simulation Conference. Abu Dhabi, UAE.*, 1, 333–346.

Aziz, K. and Durlofsky (2005). Notes for petroleum reservoir simulation. *Stanford University, Stanford, Califormia, USA.*

Brouwer, D., Jansen, J., et al. (2004). Dynamic optimization of waterflooding with smart wells using optimal control theory. *SPE Journal*, 9(04), 391–402.

Capolei, A., Suwartadi, E., Foss, B., and Jørgensen, J.B. (2013). Waterflooding optimization in uncertain geological scenarios. *Computational Geosciences*, 17(6), 991–1013.

Capolei, A., Suwartadi, E., Foss, B., and Jørgensen, J.B. (2015). A mean–variance objective for robust production optimization in uncertain geological scenarios. *Journal of Petroleum Science and Engineering*, 125, 23–37.

Capolei, A., Völcker, C., Frydendall, J., and Jørgensen, J.B. (2012). Oil reservoir production optimization using single shooting and ESDIRK methods. *IFAC Proceedings Volumes*, 45(8), 286–291.

Chen, C., Wang, Y., Li, G., and Reynolds, A.C. (2010). Closed-loop reservoir management on the brugge test case. *Computational Geosciences*, 14(4), 691–703.

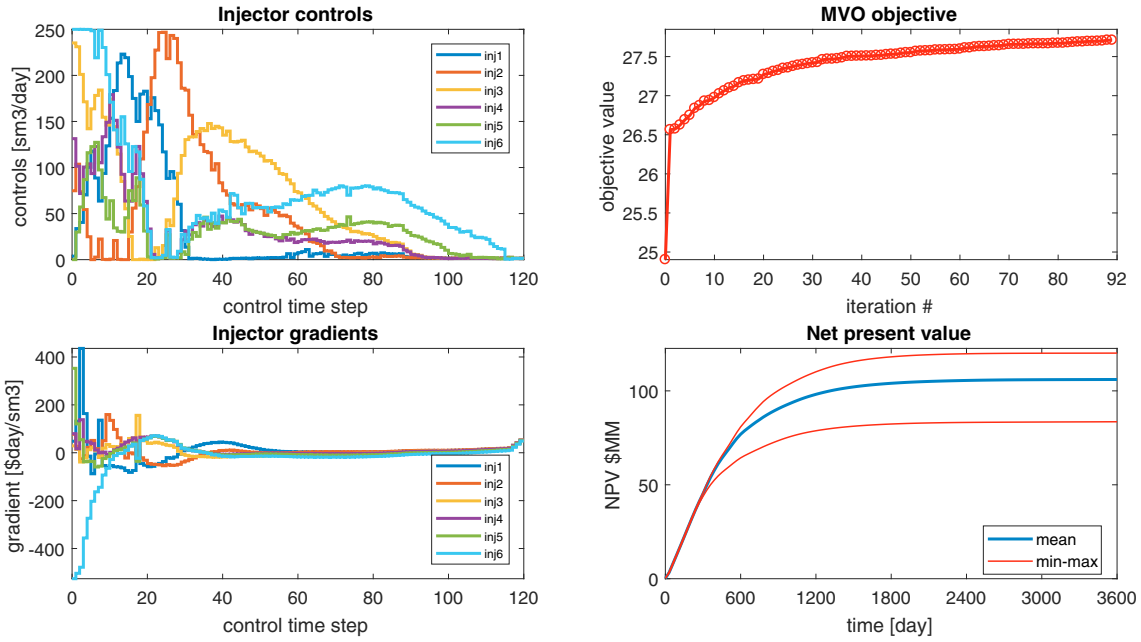

Fig. 3. The dashboard with key performance indicators for the trade-off parameter $\lambda = 0.3$. The dashboard shows the optimal water injection rates and the corresponding gradients of the objective wrt the water injection rates (left column). It also shows the mean-variance optimization criterios as function of the iteration number and the optimal evolution of the mean net present value along with the evolution of the minimum and maximim net present value (right column).

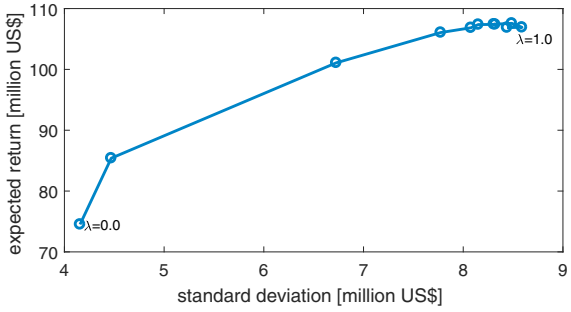

Fig. 4. The efficient frontier for the mean-variance optimization.

Chen, Z., Huan, G., and Ma, Y. (2006). *Computational methods for multiphase flows in porous media*. SIAM.

Foss, B. (2012). Process control in conventional oil and gas fields - challenges and opportunities. *Control Engineering Practice*, 20, 1058–1064.

Hanea, R.G., Fonseca, R.M., Pettan, C., Iwajomo, M.O., Skjerve, K., Hustoft, L., Chitu, A.G., and Wilschut, F. (2016). Decision maturation using ensemble based robust optimization for field development planning. In *ECMOR XV-15th European Conference on the Mathematics of Oil Recovery*.

Hou, J., Zhou, K., Zhang, X.S., Kang, X.D., and Xie, H. (2015). A review of closed-loop reservoir management. *Petroleum Science*, 12, 114–128.

Jansen, J.D., Douma, S.D., Brouwer, D.R., Van den Hof, P.M.J., Bosgra, O.H., and Heemink, O.H. (2009). Closed loop reservoir management. *SPE Reservoir Simulation Symposium. The Woodlands, Texas, USA*, (SPE 119098-MS).

Leeuwenburgh, O., Chitu, A.G., Nair, R., Egberts, P.J.P., Ghazaryan, L., Feng, T., and Hustoft, L. (2016). Ensemble-based methods for well drilling sequence and time optimization under uncertainty. In *ECMOR XV-15th European Conference on the Mathematics of Oil Recovery*.

Oliveira, D.F. and Reynolds, A. (2015). Hierarchical multiscale methods for life-cycle production optimization: A field case study. *SPE Reservoir Simulation Symposium*, (SPE-173273-MS).

Peters, L., Arts, R., Brouwer, G., Geel, C., Cullick, S., Lorentzen, R.J., Chen, Y., Dunlop, N., Vossepoel, F.C., Xu, R., et al. (2010). Results of the brugge benchmark study for flooding optimization and history matching. *SPE Reservoir Evaluation & Engineering*, 13(03), 391–405.

Rahmawati, S.D., Whitson, C.H., Foss, B., and Kuntadi, A. (2012). Integrated field operation and optimization. *Journal of Petroleum Science and Engineering*, 81, 161–170.

Sarma, P., Durlofsky, L.J., and Aziz, K. (2008). Computational techniques for closed-loop reservoir modeling with application to a realistic reservoir. *Petroleum Science and Technology*, 26(10-11), 1120–1140.

van Essen, G., Zandvliet, M., Van den Hof, P., Bosgra, O., Jansen, J.D., et al. (2009). Robust waterflooding optimization of multiple geological scenarios. *SPE Journal*, 14(01), 202–210.

Völcker, C., Jørgensen, J.B., and Stenby, E.H. (2011). Oil reservoir production optimization using optimal control. In *Decision and Control and European Control Conference (CDC-ECC), 2011 50th IEEE Conference on*, 7937–7943. IEEE.

Wang, C., Li, G., Reynolds, A.C., et al. (2009). Production optimization in closed-loop reservoir management. *SPE Journal*, 14(03), 506–523.